Accepted for publication in *Review of Scientific Intruments* **65**(11). SRF 940419-03

Design of a High-Speed, High-Resolution Thermometry System for 1.5-GHz Superconducting Radio-Frequency Cavities

Jens Knobloch, Henry Muller, and Hasan Padamsee
Floyd R. Newman Laboratory of Nuclear Studies
Cornell University, Ithaca, N.Y. 14853

November 1994

Presented in this paper are the description and the test results of a new stationary thermometry system used to map the temperature of the outer surface of 1.5-GHz superconducting single cell cavities during operation at 1.6 K. The system comprises 764 removable carbon thermometers whose signals are multiplexed and scanned by a Macintosh computer. A complete temperature map can be obtained in as little as 0.1 seconds at a temperature resolution of about 0.2 mK. Alternatively, it has been demonstrated that if the acquisition time is increased to several seconds, then a temperature resolution on the order of 30 μK is possible. To our knowledge these are the fastest acquisition times so far achieved with L-band cavities at these resolutions.

1 Introduction

Over the last decade much progress has been made in the development of superconducting radio frequency (SRF) cavities designed to be used in accelerators such as at CEBAF. In the SRF group at Cornell, peak surface electric fields of 30 and 40 MV/m (6 – 8×10^4 A/m peak magnetic fields) are routinely achieved with niobium L-band (1.5-GHz) cavities. In the case of the smaller S-band (3-GHz) cavities, even 100 MV/m has been attained.[1]

However, field levels achieved in present day cavities fall far short of those considered theoretically possible. The theoretical maximum is believed to correspond to the magnetic field at the surface reaching the superheating rf critical field of niobium (about 1.6×10^5 A/m) at which point the niobium becomes normal conducting. In reality one finds that dissipation of rf power increases drastically before this maximum field is approached, leading to a large degradation of the cavity quality (Q_0). Frequently one is therefore limited to magnetic field levels of 8×10^4 A/m or less.

Several mechanisms responsible for this Q_0 degradation have been identified and are discussed in many references. The most common mechanisms in current cavities are *thermal breakdown* and *field emission*.[2,3]

Thermal breakdown generally results when a defect, like a foreign particle, causes unusually high power dissipation in some region of the inner cavity surface. The deposited energy ultimately drives a large portion of the cavity into the normal state, thereby spoiling the Q_0.

In the case of field emission (FE), rf power is lost to electrons that tunnel out of the niobium at very localized points. The electrons are accelerated by the electromagnetic fields and, upon impact with the cavity walls, deposit their energy in the form of heat that in turn may initiate thermal breakdown. Attempts to model field emission resulted in the development of the modified Fowler–Nordheim model.[4]

Even at low field levels (below a few MV/m peak electric field) all cavities display an anomalous behavior. Although neither thermal breakdown nor FE is active at these field levels, the Q_0 of cavities is typically only 10^{10}. Calculations[2] based on the BCS rf surface resistance (R_s) of high-purity niobium (R_s = 1.5 nΩ at 1.5 GHz and 1.5 K) indicate Q_0 should be about 10^{11}. The discrepancy between this and the measured values is attributed, in part, to a high R_s due to *flux trapping*,[5] but this may be just one of many loss mechanisms.

To advance present-day accelerator technology, it is imperative to understand these cavity defects so that we may ultimately learn how to eliminate them or at least how to reduce their number. One very successful scheme used so far in the study of cavity defects

has been thermometry. The generic setup consists of an array of thermometers placed on the outer surface of the cavity so that they are sensitive to the heating produced by defects. The thermometers typically are carbon resistors specially prepared to insulate them from the helium bath, yet allowing them to be in thermal contact with the cavity surface. Below 4.2 K, the exponential increase of the thermometers' resistance with decreasing temperature allows for sensitive measurements. Thermometry systems, such as CERN's rotating system, have been used extensively in the past as powerful diagnostic tools and their success has been demonstrated in many instances. It has, for example, been possible to locate thermal-breakdown sites, some of which were found to be a result of defective electron beam welds along the equator. Many could subsequently be repaired, thereby improving the performance of the cavity. The term "guided repair" was coined for this procedure.

Overviews of the status of thermometry systems are provided in numerous papers,[6,7] and will not be repeated in detail here. However we should mention two different types that were developed at Cornell University, since their virtues were incorporated in the new system described in this report.

The first is a high-accuracy system[8] that involved the mounting of 100 sensors on the endplate of a cylindrical TE_{011} cavity. The resistance of the thermometers was measured using a lock-in amplifier in conjunction with an AC bridge circuit. The temperature resolution attainable was on the order of 1 μK at a bath temperature of 1.43 K. However, it took about 20–50 minutes to acquire a complete temperature map. Drifts in the bath temperature therefore could compromise the system's performance and studies of transient effects were impossible.

To improve upon the scan times, a high-speed system was also developed at Cornell.[9] This used an array of 684 demountable thermometers attached to an L-band cavity. An intricate matrix scheme in the helium space was employed so that only 56 leads were required to be fed into the cryostat. These were scanned by a multiplexer controlled by a PDP-11 computer which required 15 seconds for the acquisition of a complete map at a temperature resolution of approximately 5 mK. However, due to the matrix scheme and numerous cross talk problems, it frequently proved difficult to distinguish between genuine temperature signals and artificial ones that were caused by defective leads or thermometers.

In view of our past success with thermometry, we recently built a new system that was designed to incorporate both the high sensitivity and the rapid scan capabilities of the previous Cornell systems.

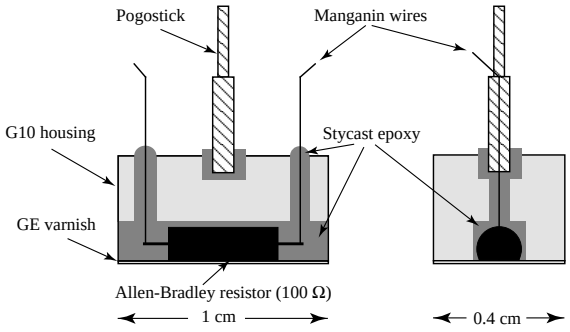

Figure 1: Schematic of a single thermometer. In total 764 thermometers are required for the temperature mapping system.

2 System Design

The thermometers used are identical to the ones employed by the old Cornell rapid scan system. A schematic is shown in Figure 1.

The temperature sensing element is a 100 Ω Allen-Bradley resistor set in G-10 and encased by epoxy (Stycast 2850 FT). Manganin wires, 0.14 mm in diameter, are spot welded to the resistor contacts and used as leads to reduce the cooling of the resistor by the helium bath. One of the broad surfaces of the thermometer is ground away until the carbon element of the resistor is exposed after which the element's electrical insulation is restored by coating it with a thin layer of GE-varnish (7031). A spring-loaded pin ("pogo stick") is mounted on the opposite side of the G-10 casing and provides a contact force of about 2 N between the thermometers and the cavity surface. Twenty-one thermometers are inserted into 21 equidistant holes in G-10 boards ("thermometer boards") machined to match the contour of the cavity, as is shown in Figure 2(a). Printed circuitry on the thermometer boards is used to simplify the wiring scheme. The boards are attached to the cavity as shown in Figure 2(b), thereby bringing the thermometers in contact with the surface.

Apiezon N grease is used as a bonding agent between the thermometer and the wall to prevent superfluid helium from reaching and cooling the exposed carbon element. Altogether 36 thermometer boards, spaced by 10°, are used to cover the cavity with a total of 756 thermometers. Seventy-two more thermometers are used by this system than the old Cor-

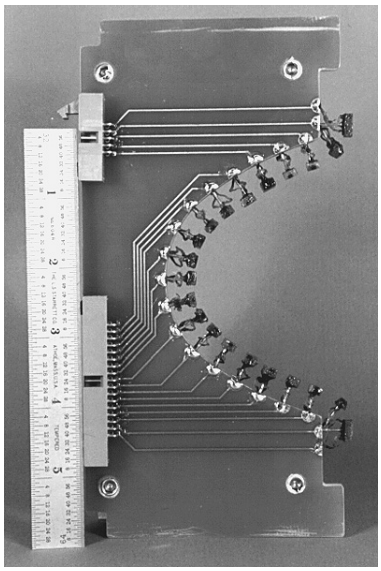

(a)

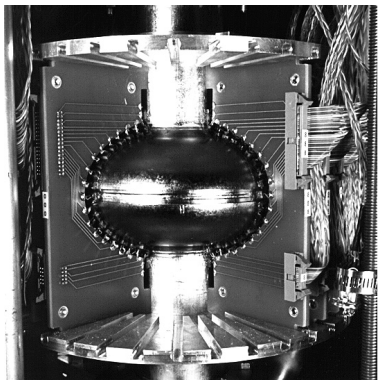

(b)

Figure 2: Photograph of (a) a single thermometer board and (b) several boards mounted on the cavity.

nell high-speed system, because 36 additional thermometers are attached around both the top and bottom beam tubes near the iris. In the past, it was found that heating due to field emission can be significant in these regions.

The spacing between thermometers on neighboring boards varies from about 0.65 cm at the iris to 1.7 cm at the equator, whereas the spacing along a board is 0.85 cm. Calculations and experiments have shown that the width of the temperature distribution due to a point heat source should have a FWHM of about 0.8 cm at the outer cavity surface at 1.6 K. Thus, generally, we expect that at least two thermometers should always respond to heating on the cavity interior, provided the dissipated power is sufficient to be measurable.

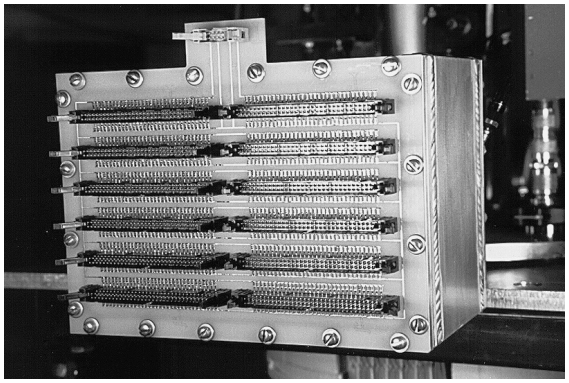

Figure 3: Photograph of one of the two 768-lead feedthroughs attached at the top of the test stand.

An additional 8 thermometers are suspended in the helium bath without being in contact with the cavity. These are used to monitor the bath temperature, allowing us to compensate for thermal drifts during the acquisition of a temperature map. Thus a total of 764 thermometers needs to be scanned.

At 1.6 K, which presently is the lowest temperature we can reach with our pumping system, the resistance of the thermometers is typically about 12 kΩ and their sensitivity $\Delta R/\Delta T$ is approximately 33 Ω/mK.

To permit great independence in the wiring within the cryostat, each thermometer has two sense leads which also serve as the current leads within the cryostat. Outside the cryostat the sense leads are connected to a multiplexing scheme. We use independent leads for each thermometer to guarantee that only one thermometer is affected should a wire or connection in the cryostat fail. In the previous Cornell high-speed system, most leads were shared by several thermometers so that up to 55 thermometers could be affected by a wire failure.

However the independence comes at a cost. Using the wiring scheme detailed below, 1528 leads need to be fed into the 6 torr helium space in which the cavity is operated. We designed two large feedthroughs, as shown in Figure 3, to take care of this. They consist of two $16.5 \times 23.6 \times 12.7$ cm^3 aluminum boxes that are bolted onto rectangular flanges leading into the cryostat via rectangular vacuum tubes. Each of the boxes has a demountable brace at the front side, needed to support the pressure acting on the feedthrough. The feedthrough itself consists of a demountable 16.5×23.6 cm^2, 0.32 cm thick G-10 board with 768 plated through holes. Twelve 64-

pin printed-circuit-board headers with 1.55 cm long tail pins are inserted in these holes and soldered in place. The solder is sufficient to maintain a vacuum of better than 1 torr. Furthermore, each of the two G-10 boards holds the appropriate circuitry for parallel operation of the thermometers. The key components of these circuits are 768 1 MΩ chip resistors on each board, of which always two in conjunction with the driving voltage act as a current source for one thermometer. The chip resistors also isolate the thermometers from each other, thereby eliminating ground loop problems. The entire grid is driven by a Keithley 230 voltage source controlled via GPIB by a Macintosh Quadra 700.

Twelve twisted pair ribbon cables (28 gauge) are attached to the long tails on the interior of each feedthrough box using conventional insulation-displacement-connectors (IDC's) and are fed by way of the rectangular vacuum pipe into the cryostat. There they are attached, again using IDC's, to the appropriate thermometer board. Should a cable fail, it is fairly straight forward to detach it from the feedthrough and to insert a new one. There was some concern that the IDC's were prone to failure in superfluid helium, but that has not been the case so far. The total heat leak through these wires into the helium liquid was found to be at most 1–2 W.

On the air side of the feedthrough, IDC's connect to 2-meter-long shielded, twisted pair, ribbon cables which lead to the multiplexing system. To scan the numerous signals, we have adopted the SCXI^{TM} system from National Instruments. This consists of two chassis placed outside the radiation shielding of the test area. Both chassis contain twelve SCXI-1100 modules, each of which is capable of multiplexing 32 differential inputs, allowing us to scan 768 signals. Furthermore, the SCXI-1100 modules amplify the multiplexed signals using gains of 1–2000 before they are routed to the Macintosh (about 3.5 m away), where the signal is digitized by a National Instruments NB-MIO 16XL 16 bit analog to digital converter (ADC). The specified maximum rate between conversions is 24 kHz. A National Instruments direct memory access board (DMA-2800) is used in conjunction with the ADC to free up the computer's CPU for other tasks. The control code is written using National Instrument's LabVIEW^{TM} programming language.

The wiring between the feedthrough and the SCXI chassis is arranged in such a manner that neighboring thermometers are always scanned sequentially in time. This results in a somewhat awkward wiring scheme, however it resolves any cross talk problems that could otherwise occur due to settling times in the amplifiers on the multiplexer cards. The effective source impedance of the voltages being measured nearly equals the resistance of the thermometers which at 1.6 K is about 12 kΩ. We found that for the largest voltage jumps anticipated, the amplifiers settle to within 99.995% of the true value within the scan interval, provided we operate within the specifications of the ADC. In this case settling problems would not become apparent unless we operate the thermometry system at resolutions better than 20 μK. However, if we were to work at 1.4 K (which we hope to do someday) the source impedance would increase to up to 40 kΩ and settling times become an issue. If channels are switched at a rate of 21 kHz the amplifiers would only settle to within 99% of the final value for a 40 kΩ thermometer that is scanned directly after a "hot" one that registers more than 2 K above ambient (i.e., whose resistance is around 1 kΩ). A spurious temperature signal of about 8 mK would hence result in the temperature map. At a scan rate of 10 kHz this artificial signal is reduced to about 0.4 mK. However, since the neighbors of the "hot" thermometer are heated by the same source to a temperature significantly greater than a few millikelvin, any artificial signals are swamped provided a warm neighbor is scanned immediately following the "hot" thermometer.

During the acquisition of a temperature map, the computer measures the average voltage across each thermometer by scanning the thermometers several times. It then switches the polarity of the drive source and repeats the process before taking the difference between the two sets of measurements. These values allow the computer to calculate the resistance of each thermometer. The reversal of polarity is needed to cancel out any contact voltages in the circuits and offsets in the amplifiers. If the number of scans at each polarity is limited to one, the entire scanning process takes about 0.1 seconds, a factor of 150 faster than the previous Cornell high-speed system. On the other hand, if we are willing to sacrifice some acquisition speed for an improvement in resolution, we can easily increase the number of scans over which we average.

A calibrated LakeShore germanium thermometer (GR-200A-250) is also included in the helium bath. It serves as a reference for the cross calibration of the carbon thermometers as the helium bath is cooled from 4.2 to 1.6 K at the outset of a test. Typically, calibration points are taken at about 0.1 K intervals,

using the scanning scheme outlined above. Once the calibration measurements are completed the data is approximated by a curve of the form

$$\frac{1}{T} = a + bx + cx^2 + dx^3; \qquad x = \ln(R) \qquad (1)$$

where T is the temperature, R is the thermometer resistance, and a, b, c and d are fit parameters. At that point the system is ready to map the temperature distribution of the cavity. A complete map is obtained by scanning the voltages of the individual resistors as outlined above, once with the rf power switched on and once with it switched off. It is the difference in temperature (ΔT) that the computer then calculates from the measured thermometer resistances. This procedure is employed to cancel out the bath temperature and the self heating of the thermometers due to the excitation voltage. If desired, the user can also map the cavity several times in rapid succession to study transients or a sub region of the cavity can be mapped to investigate individual sites of interest.

Extensive studies have been performed on the efficiency of the thermometers.[10] The efficiency η is defined as the ratio of the measured temperature rise to the calculated temperature rise at the cavity's outer surface. Generally we found that η was around the 30% mark with perhaps a 20% spread in this value. The response of the thermometers versus dissipated power was found to be essentially linear[10] in the range of 1 μK to 1 K.

A study of the self heating of the thermometers as a function of excitation voltage revealed that it is quadratic, as can be expected for ohmic heating. A temperature rise of approximately 1 mK was detected for a power dissipation of 0.2 μW due to the excitation voltage. On the other hand, during our experiments we could easily detect temperature rises of 0.1 mK or less due to external heat sources. Although this is significantly less than the self heating, the latter is easily calibrated out since all measurements are designed to yield the temperature difference between the cavity in operation and the cavity being switched off. However, for self heating greater than the 1 mK level we found that the measured signals were severely swamped, thereby compromising the sensitivity of the system.

Besides controlling the temperature mapping system, the Macintosh also runs a second setup which measures the cavity Q_0 as a function of the peak electric field ($E_{\rm pk}$). The generic design of such a system has been described elsewhere.[2,11]

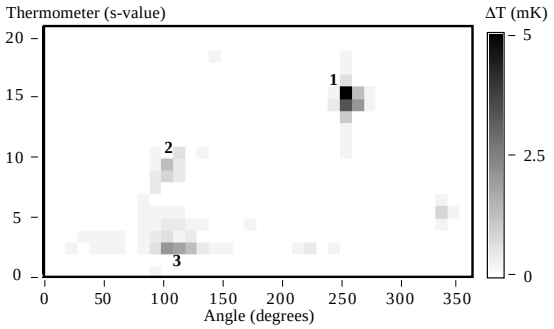

Figure 4: "Unfolded" temperature map of the cavity at a peak electric field of 4.5 MV/m. The upper iris of the cavity corresponds to $s = 19$, the equator to $s = 10$ and the lower iris to $s = 1$ in the map, where s is the thermometer number along a given azimuth. For an idea of how this map corresponds to the true cavity surface, refer to Figure 7.

3 Test of the System & Discussion

The capabilities of the system were tested using a 1.5-GHz niobium cavity, 0.32 cm thick, with a residual resistivity ratio of 180. The cavity was cleaned in an ultrasound agitator using ultrapure deionized water. A chemical etch, which is generally performed on such cavities,[12] was omitted in this case to ensure that numerous dissipative sites would exist during cavity operation.

The thermometers' excitation voltage was about 35 mV, resulting in a power dissipation of approximately 0.1 μW in each thermometer. The measured voltages were amplified at the SCXI chassis by a factor of ten and a second amplifier on the ADC board in the Macintosh boosted the signal yet another 10 times to about 3.5 V.

Measurements of the cavity's Q_0 as a function of $E_{\rm pk}$ yielded $Q_0 = 5{\times}10^9$ until a field of 14 MV/m was reached. X rays were initially detected at 12.5 MV/m peak electric field by a counter placed on the outside of the cryostat, thereby indicating the onset of field emission. Above 14 MV/m the Q_0 began to dip, dropping rapidly to about 5×10^8 at 18 MV/m.

Since Q_0 is roughly constant at low fields we expect only to find Joule heating below 12.5 MV/m, because these losses scale as $E_{\rm pk}^2$, just like the stored energy. This observation is indeed borne out by the temperature data. Figure 4 depicts a typical temperature map taken at $E_{\rm pk} = 4.5$ MV/m. Three sites of significant heating were detected and they

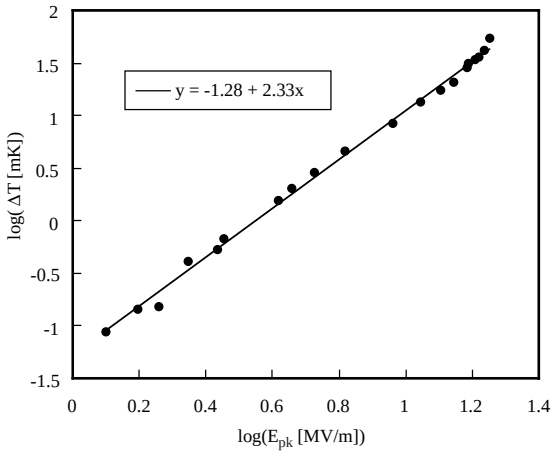

Figure 5: Log-log plot of the heating at site 2. The linear dependence indicates that the heating follows a power law as a function of electric field. If the heating was purely due to Joule losses, the slope should be two.

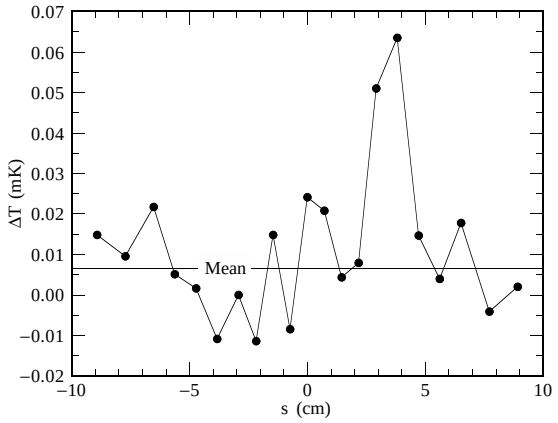

Figure 6: Temperature profile at fixed azimuth ($\phi = 250°$). The peak at $s = 4$ cm corresponds to the heating at site 1. The signal is about six standard deviations above the background noise. The peak electric field was 0.7 MV/m.

display characteristics consistent with Joule heating due to the magnetic field. The fact that two of these sites are near the equator, where the magnetic field is strong (the cavity is operated in the TM_{010} mode) is one indicator of this. Another is that a log-log plot (Figure 5) of the heating of, for example, site 2 versus $E_{\rm pk}$ yields a straight line with slope 2.33 ± 0.05 confirming essentially ohmic losses. If the heating were purely due to Joule heating this slope should be two. Hence there are indications that additional, unexplained processes may be active. Such behavior, which cannot be modeled by either Joule heating or field emission alone, has been observed in other experiments as well.[1,13]

Similarly, site 1 also shows the characteristics of Joule heating. A temperature profile, taken along that site's longitude, shows that we were easily able to detect heating at the 65 μK level, as can be seen in Figure 6.

At this resolution it takes approximately 2.5 seconds to map the entire cavity (not counting the time required for the "rf power off" scanning and any post scan processing). The standard deviation (σ) of the noise (i.e., all thermometers except the three nearest $s = 4$ cm) is 10 μK, which is about 170 times better than the previous Cornell high-speed system. Calculations indicate that at the 3σ level it would be possible to detect the heating of 0.32 cm thick niobium with a surface resistance of 1.5 nΩ, if it were exposed to a magnetic field of 8300 A/m. This surface resistance is comparable to the theoretical $R_{\rm s}$ of high-purity niobium. Magnetic field levels of 8300 A/m require peak electric fields of 4.1 MV/m in our cavities, which can easily be achieved. Thus, at the temperature resolutions we have attained, we can study any departures in surface resistance from the theoretical $R_{\rm s}$.

If, on the other hand, the acquisition time is reduced to about 0.1 s (i.e. the number of samples over which we average is diminished) then the 3σ level of the noise increases to around 0.2 mK. In that case we are sensitive to an $R_{\rm s}$ of 10 nΩ in an 8300 A/m field.

Above about 12.5 MV/m peak field, we expect the exponentially rising field emission to begin dominating the cavity losses, as indicated by the measured drop of Q_0. The temperature map obtained at 17.2 MV/m (Figure 7) clearly shows that several new sites near the iris have appeared. These are the regions where the electric field is strongest and field emission is to be expected. A plot of temperature rise versus peak field for site 7 clearly shows how the emitter is dormant until a threshold field of about 16 MV/m is exceeded (Figure 8).

Once emission begins, it rises exponentially with increasing field. Theoretical treatments of field emission,[3,14] predict that the emitted current should go as

$$I = C\frac{A}{\Phi}(\beta E)^2 \exp\left(-B\frac{\Phi^{1.5}}{\beta E}\right) \qquad (2)$$

where E is the local electric field, Φ is the work function at the site (4 eV for pure niobium), A is the effective area of the emission site, β is the local field

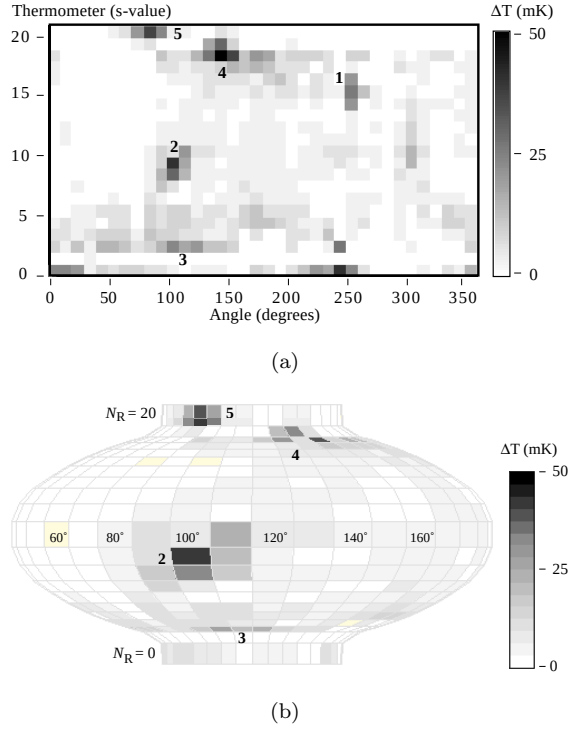

Figure 7: (a) "Unfolded" temperature map of the cavity obtained at a peak electric field of 17.2 MV/m. (b) 3-D representation of the cavity showing part of the same temperature distribution as in (a).

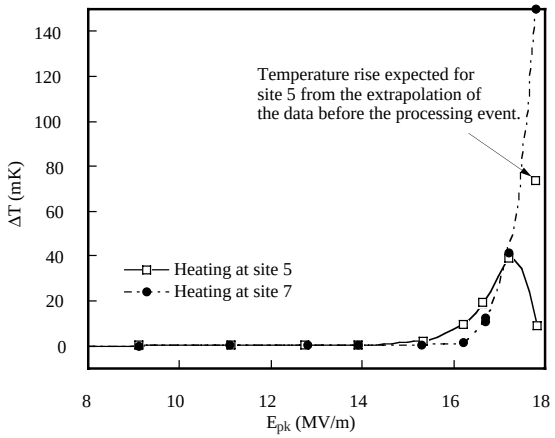

Figure 8: Heating at sites 5 and 7 as a function of peak electric field. Field emission-like behavior is displayed by the fact that heating does not occure until a threshold field is exceeded after which the heating increases exponentially. Site 5 processed, as indicated by the reduction in heating at 17.8 MV/m. An extrapolation of the curve before processing shows that the heating should have been 74 mK had the site not processed away.

enhancement factor and C and B are material dependent constants.

The total power dissipated by the emitted electrons upon impact at some other point of the cavity wall is expected to scale approximately as in (2). A plot of $\ln(\Delta T/E_{\rm pk}^2)$ versus $1/E_{\rm pk}$ should thus yield a straight line, which indeed turns out to be true for site 7 above 16 MV/m. β, being inversely proportional to the slope, was found to be 96, which is consistent with typical β values of emission sites in many cavities.[3]

Site 5 proved to be particularly interesting. This site "processed" once a field level of 17.2 MV/m was exceeded. The term "processing" refers to the fact that the field emission was irreversibly reduced at a given field level. Figure 8 depicts the heating of the site as a function of peak field, the sudden dip at $E_{\rm pk} = 17.8$ MV/m being very apparent. An extrapolation of the curve before the processing event indicates the heating should have been 74 mK if the site had not processed. Unfortunately we did not measure ΔT versus $E_{\rm pk}$ after the processing event during this test. However in a subsequent run that was performed after the cavity was thermally cycled to room temperature, we did measure the emitter's characteristics and it was found that field emission was all but eliminated at that site, whereas all the other sites were still active.

4 Further Projects

The map in Figure 7 also brought to light one of the problems of the thermometry system. We see that the thermometers at $s = 1$ (at the lower iris) show little response although some neighboring thermometers register significant heating. We believe the main cause of this lies in the fact that the iris' radius of curvature is very tight and it is difficult to make good contact between the thermometers and the cavity wall, especially if thermometer boards are not centered properly with respect to the cavity equator. Currently we are trying to design a series of heaters which we are planning to attach to the beam tube of the cavity. These would allow us to determine the efficiency of the iris thermometers.

Sites, such as the one that processed (site 5) are of particular interest to us. We have begun developing a method of cutting the niobium cavity cleanly into 8 segments, which individually are able to fit in our scanning electron microscope (SEM) for examination. We intend to analyze the appearance of such sites using the thermometry data to pinpoint their

location. Incorporated in our SEM is an energy ispersive x-ray system which permits us to probe the elemental composition within the first micron of the surface. To achieve a greater surface sensitivity we are prepared to resort to Auger electron spectroscopy. The successful localization of defects in an SEM using thermometry as a guide has been demonstrated to be feasible in 3-GHz S-band cavities.[1] We believe we have the capabilities to do the same with L-band cavities.

Since the new system is so fast, we have a powerful tool to study transients in power dissipation. We have, for example, been able to follow in detail the heating of several sites as the rf power is switched on and the cavity fills. Fill times are on the order of 1/2 second and the system can easily acquire several maps in that period. We were thus able to produce a "movie" of the cavity temperature which clearly shows at what times various heat sources became active. It is also our hope to study by these means the transient behavior of defects as they process away.

One of the advantages of the new system is that the 1.5-GHz cavities have a four times larger surface area than the 3 GHz cavities previously used at Cornell for the SEM examination of defects. Furthermore the L-band geometry permits a slightly denser array of thermometers. We thus expect that we will be able to obtain more data per test and hope to gather rapidly reliable statistics on the behavior, physical appearance, and chemical composition of cavity defects. Armed with this information we ultimately hope to learn about the nature of the defects and the mechanisms involved in rf power dissipation.

5 Acknowledgments

We would like to thank Nicholas Black and Gautam Parthasarathy for manufacturing many of the thermometers and work on miscellaneous parts of the test stand.

References

[1] J. H. Graber, *High Power Processing Studies of 3 GHz Niobium Superconducting Accelerator Cavities*, PhD thesis, Cornell University, 1993, Laboratory of Nuclear Studies thesis CLNS 93-1.

[2] H. Piel, Superconducting cavities, in *CERN Accelerator School: Superconductivity in Particle Accelerators*, edited by S. Turner, pages 149–196, Hamburg, Germany, 1988, CERN publication 89–04.

[3] H. Padamsee, Superconducting rf, in *The Physics of Particle Accelerators*, edited by M. Month and M. Dienes, pages 1403–1482, American Institute of Physics, 1992, AIP Conference Proceedings 249.

[4] H. A. Schwettman, J. P. Turneaure, and R. F. Waites, *Journal of Applied Physics* **45**, 914 (1974).

[5] C. Vallet et al., Flux trapping in superconducting cavities, in *Proceedings of the 1992 European Particle Accelerator Conference*, edited by H. Henke, H. Homeyer, and C. Petit-Jean-Genaz, pages 1295–1297, Berlin, Germany, 1992.

[6] H. Piel, Diagnostic methods of superconducting cavities and identification of phenomena, in *Proceedings of the Workshop on RF Superconductivity*, edited by M. Kuntze, pages 85–118, Karlsruhe, 1980, Proceedings also published as internal Kernforschungszentrum Kalsruhe report KFK-3019.

[7] C. E. Reece, Progress in diagnostic techniques for sc cavities, in *Proceedings of the 3rd Workshop on RF Superconductivity*, edited by K. W. Shepard, pages 545–563, Argonne, Illinois, 1988, Proceedings also published as internal Argonne report ANL-PHY-88-1.

[8] P. Kneisel, G. Müller, and C. Reece, *IEEE Transactions on Magnetics* **MAG-23**, 1417 (1987), Proceedings of the 1986 Applied Superconductivity Conference.

[9] H. Padamsee et al., Field emission studies in superconducting cavities, in *Proceedings of the 1987 IEEE Particle Accelerator Conference*, edited by E. R. Lindstrom and L. S. Taylor, pages 1824–1826, Washington D.C., 1987.

[10] G. Müller and P. Kneisel, Development of sensitive thermometers for calibrated surface temperature measurements of niobium cavities immersed in superfluid helium, Technical report, Cornell University, Laboratory of Nuclear Studies, 1985, SRF report 851291 EX.

[11] J. Knobloch, Basic concepts of measurements made on superconducting rf cavities, Technical report, Cornell University, Laboratory of Nuclear Studies, 1991, SRF report 910927-07.

[12] P. Kneisel, Surface preparation of niobium, in *Proceedings of the Workshop on RF Superconductivity*, edited by M. Kuntze, pages 27–40, Karlsruhe, 1980, Proceedings also published as internal Kernforschungszentrum Kalsruhe report KFK-3019.

[13] R. W. Röth et al., Anomalous loss mechanisms in high purity Nb cavities, in *Proceedings of the 5th Workshop on RF Superconductivity*, edited by D. Proch, pages 599–615, Hamburg, Germany, 1991, Proceedings also published as internal DESY report DESY M-92-01.

[14] R. Noer, *Applied Physics* **A 28**, 1 (1982).